

An edited version of this paper was published by [AGU](#).

---

## Remotely forced biweekly deep oscillations on the continental slope of the Gulf of Guinea

Catherine Guiavarc'h<sup>1,\*</sup>, Anne Marie Treguier<sup>1,\*</sup>, Annick Vangriesheim<sup>2</sup>

<sup>1</sup> Laboratoire de Physique des Océans, Ifremer, Plouzané, France

<sup>2</sup> Laboratoire Environnement Profond, Ifremer, Plouzané, France

\*: Corresponding author : Guiavarc'h Catherine, email address : [catherine.guiavarch@ifremer.fr](mailto:catherine.guiavarch@ifremer.fr) ; Treguier Anne Marie, email address : [Anne.Marie.Treguier@ifremer.fr](mailto:Anne.Marie.Treguier@ifremer.fr)

---

### Abstract:

Current meter measurements on the continental slope of the Gulf of Guinea (at 7°20'S and 1300 m depth) have revealed biweekly oscillations of the currents, bottom intensified and oriented along the bathymetry. We develop a three-dimensional primitive equation model of the Gulf of Guinea to study the oscillations and their forcing mechanism. The high resolution (1/12°) regional model reproduces remarkably well the main characteristics of the deep currents on the continental slope. Experiments with different forcings demonstrate that the biweekly variability at 1300 m depth is remotely forced by equatorial winds. Deep Yanai waves generated by the wind propagate eastward along the equator. Upon reaching the African coast, the energy propagates poleward in both directions as coastal trapped waves. The selection of the dominant biweekly period is explained by the absence of equatorial waves with westward group velocities in that frequency band. Contrary to a previous hypothesis involving tidal forcing, our interpretation is coherent with the significant interannual variability of the biweekly energy.

**Keywords:** Coastal trapped waves; numerical modeling; Gulf of Guinea

## 1. Introduction

21 There has been recently a renewed interest for the intra-seasonal variability in the  
22 tropical Atlantic, both in the atmosphere and in the ocean. The African monsoon is char-  
23 acterized by significant variability of rainfall as well as winds at periods between 10 and 60  
24 days (*Janicot* [2001]). Biweekly oscillations of the winds are emphasized by *Grodsky and*  
25 *Carton* [2001] as well as *Mounier and Janicot* [2004]; the associated modes of variability  
26 cover the whole tropical Atlantic, from the Gulf of Guinea to the intertropical convergence  
27 zone. In the equatorial band the variability of surface winds is the main driving mech-  
28 anism for the ocean, and indeed oceanic variability is found in the equatorial Atlantic  
29 ocean at periods between 10 and 60 days. *Garzoli* [1987] used inverted echo sounders  
30 to document oscillations of the upper thermocline and their relationship with the atmo-  
31 spheric variability. Recently *Bunge et al.* [2006] analyzed current meter measurements at  
32 10°W along the equator. They found variability at periods ranging from 5 to 40 days,  
33 down to a depth of 1500 m, and suggested that the wind is probably the most important  
34 driving mechanism for periods shorter than 20 days.

35 In the deep ocean farther south (at 7°20'S), biweekly current oscillations have been  
36 observed recently on the continental slope off Angola (*Vangriesheim et al.* [2005]). The  
37 measurements were carried out during the Ifremer (Institut Francais de Recherche pour  
38 l'Exploitation de la Mer) pluridisciplinary program so-called BIOZAIRE, whose main  
39 focus was the study of benthic ecosystems. Long term moorings of sediment traps and  
40 current meters have been installed near the sea floor between years 2000 and 2003, in a  
41 water depth of 1300 m (Fig. 1). Four year time-series of current velocities at 30 m above

the bottom are shown in Fig. 2. The currents exhibit remarkable biweekly oscillations, with a peak-to-peak amplitude of 20-30 cm/s, which completely dominate the signal at sub-inertial frequencies. The oscillations are bottom-intensified and clearly oriented along the bathymetry, which is why *Vangriesheim et al.* [2005] have tried to explain them in terms of linear topographic waves. The Coastal Trapped Waves (CTWs) model of *Huthnance* [1978] has been found the most adequate to describe the observations. This model assumes a topographic slope which is uniform in the direction of the coastline, so that the linear solution is a superposition of modes propagating along the coast, with a fixed cross-slope and vertical structure. For mode  $i$ , the velocity changes sign  $i$  times across the slope. *Vangriesheim et al.* [2005] show that modes 3 and 5 are consistent with the observed data, so that the biweekly oscillations could be explained by a superposition of CTW modes. However, they consider only the simplest model, one of free coastal trapped waves propagating along an infinite slope. Such waves exist at all sub-inertial frequencies, so that the free solutions cannot explain the selection of the biweekly frequency in the observations. Moreover, the simple model does not allow a quantitative study of the mechanisms that could generate these deep oscillations.

*Vangriesheim et al.* [2005] were the first to report biweekly current oscillations in the Gulf of Guinea at such a depth (1300 m), but biweekly variability of sea level and temperature had been observed before (in the 1970s) on the continental shelf (e.g., *Picaut and Verstraete* [1979]). At that time, tidal forcing was proposed as the most likely mechanism (*Houghton* [1979], *Clarke and Battisti* [1983]). In the present paper we explore the surface wind as a forcing mechanism for the deep biweekly oscillations observed on the BIOZAIRE site. Our approach is motivated by the new evidence for a strong biweekly

65 signal in the atmosphere, but also by preliminary results reported by *Vangriesheim et al.*  
66 [2005]. They considered a three-dimensional, primitive equations numerical model, with  
67 a  $1/6^\circ$  horizontal grid and 42 vertical levels (ATL6), forced by daily atmospheric winds,  
68 heat and freshwater fluxes from the ECMWF center. Although the model did not in-  
69 clude tidal forcing, it did reproduce biweekly oscillations, oriented along the bathymetry.  
70 The ATL6 model results were not completely satisfactory, though. The kinetic energy  
71 spectrum simulated at the BIOZAIRE site had two peaks at the 14-day and 30-day peri-  
72 ods, but the 14-day period did not dominate the signal. The amplitude of the modelled  
73 currents was lower than the observations by a factor of 5 to 10, and the bottom intensifi-  
74 cation was too weak. The main aim of the present study is to demonstrate that a regional  
75 model with improved vertical and horizontal resolution is able to reproduce the observed  
76 currents at the BIOZAIRE site, much better than ATL6. This is an important goal since  
77 the biweekly oscillations are the dominant subinertial signal at that location; their correct  
78 representation in a general circulation model is a necessary step before such models can  
79 be used in various contexts such as the study of the deep environment or the design of  
80 offshore platforms or pipelines.

81 The second section of this paper is devoted to a discussion of additional, unpublished  
82 current data at the BIOZAIRE site. Time series collected by TOTAL in 1997-1998 confirm  
83 the existence of the bottom-trapped oscillations and better document the vertical structure  
84 of the signal. We also discuss the hypothesis of tidal forcing by performing a harmonic  
85 analysis of the continuous 4-year series of deep current measurements now available at  
86 BIOZAIRE. Section 3 presents our new high resolution model of the Gulf of Guinea with  
87 a  $1/12^\circ$  horizontal grid and 100 vertical levels, which overcomes the deficiencies found

88 by *Vangriesheim et al.* [2005] in the ATL6 model. A detailed validation of the model  
89 at the BIOZAIRE site is presented in section 4. The model is then used to investigate  
90 the generation of the deep biweekly oscillations on the slope (section 5). Using a suite  
91 of sensitivity experiments we demonstrate that the oscillations are remotely forced by  
92 equatorial winds. In section 6 we study the propagation of the signal and propose a  
93 mechanism explaining the selection of the biweekly frequency.

## 2. Observations

94 The first BIOZAIRE current data at  $7^{\circ}20'S, 11^{\circ}30'E$ , fully described in *Vangriesheim*  
95 *et al.* [2005], were carried out at three depths: 410 meters above bottom (mab), 150 mab  
96 and 30 mab, from March 2000 to January 2001. Measurements at 410 mab and 30 mab  
97 are available up to February 2003. The amplitude of the oscillations varies from year to  
98 year with a maximum in 2000 (Fig. 2). The biweekly current oscillations at 30 mab are  
99 oriented almost parallel to the local isobaths although in 2003 the orientation exhibits  
100 more variability (Fig. 2). The mooring at site A near the 1300 m isobath gives informa-  
101 tion on the vertical structure of the signal (which is bottom intensified) and an additional  
102 mooring located at 4000 m near the foot of the continental rise has been used by *Van-*  
103 *griesheim et al.* [2005] to discuss the cross-slope structure of the signal. They found that  
104 the biweekly oscillations were consistent with modes 3 and 5 of CTWs. The corresponding  
105 along-slope wavelengths and phase speeds for a biweekly frequency are 1200 and 680 km  
106 and 0.9 and 0.4 m/s, respectively.

107 In addition, unpublished current data provided by TOTAL are available at approxima-  
108 tively the same location, from a mooring deployed in 1385 m water depth at  $7^{\circ}40'S, 11^{\circ}40'E$   
109 between September 1997 and October 1998. This mooring provides measurements over

110 the whole water column, with 6 Aanderaa RCM 7/8 current meters at 385 m, 585 m,  
111 785 m, 985 m, 1185 m and 1370 m below mean sea level. These new profiles will allow  
112 additional model validation.

113 Both mean velocities and eddy kinetic energy of the TOTAL mooring agree with the  
114 BIOZAIRE data (Table 1). Near the bottom, in both datasets, the mean flow is oriented  
115 to the south-east. The total eddy kinetic energy which is  $19 \text{ cm}^2 \cdot \text{s}^{-2}$  at the shallower depth  
116 (385 m), decreases to  $13 \text{ cm}^2 \cdot \text{s}^{-2}$  at 785 m and then increases to  $23 \text{ cm}^2 \cdot \text{s}^{-2}$ , its maximum  
117 value, at 1185 and 1370 m. The TOTAL data stick-plots (Fig. 3) exhibit intra-seasonal  
118 oscillations similar to the BIOZAIRE data. The orientation of the currents along the  
119 topography is not present for the shallower data, but well-marked at 1185 m and 1370 m.  
120 At the deepest level (15 mab) the current ellipse is less tight than for the BIOZAIRE  
121 measurements. The amplitude of the oscillations is smaller than those observed during  
122 the first year of the BIOZAIRE data but in good agreement with other, less energetic  
123 years as shown in Table 2. Kinetic energy spectra have been computed for all the levels  
124 and are displayed in Fig. 4. At all depths, peaks appear at a period close to 14 days.  
125 The magnitude of those peaks is nearly the same at the three shallower depths (358 m,  
126 585 m and 785 m) but increases from 985 m to the near-bottom level where the 14-day  
127 period is the most energetic. Those results confirm the previous analysis of *Vangriesheim*  
128 *et al.* [2005] who showed an intensification of the 14-day oscillations between 410 mab and  
129 30 mab. Note that contrary to the spectra displayed by *Vangriesheim et al.* [2005], we  
130 have not filtered inertial motions in Fig. 4 (the inertial period at the BIOZAIRE site is  
131 close to 4 days). The observations do not show a large signal at the inertial frequency. At

132 periods of a few days, the currents are more energetic at 385 m than in the deep layers,  
133 contrary to the biweekly period.

134 *Vangrishesheim et al.* [2005] used three years of current meter measurements; an additional  
135 year (2003) is now available at the same location, for the deepest level only (30 mab).

136 We can thus compare the kinetic energy in the frequency band around 14-day (12-17  
137 days) for four different years (Table 2). The 14-day eddy kinetic energy has a strong  
138 interannual variability since the signal in 2000 is twice as energetic as the years 2001, 2002  
139 and 2003. A wavelet analysis of the currents (*Guiavarc'h* [2007]) confirms the temporal  
140 intermittency of the 14-day signal. Those results suggest that those biweekly oscillations  
141 are not forced by the tide, since the astronomical forcing has no interannual variability.

142 *Picaut and Verstraete* [1979] calculated spectra of sea surface height time series along  
143 the northern coast of the Gulf of Guinea. Two distinct peaks appeared at the 13.7 days  
144 and 14.7 days periods, corresponding to two tidal components (Mf and MSf). *Picaut*  
145 *and Verstraete* [1979] suggested that because the direct tidal forcing at those periods is  
146 weak, the biweekly sea-level oscillations must be due to the nonlinear interaction between  
147 the higher frequency components, M2 and S2 for the 13.7 day period and M2 and K2  
148 for the 14.7 day period. We do not see such well separated peaks in the BIOZAIRE  
149 velocity spectra. Even in nonfiltered spectra (*Guiavarc'h* [2007]), there is an increased  
150 energy over a wide band (12 to 17 days). To further investigate this question, we have  
151 performed an harmonic analysis using the four years BIOZAIRE current data at 30 mab.  
152 None of the tidal components mentioned by *Picaut and Verstraete* [1979] appear to be  
153 significant, and their amplitude differs from year to year. It is quite likely that although  
154 low frequency tidal signals affect the sea surface height, they have a very small effect on

155 currents because the phase variations of the biweekly tides in the Gulf of Guinea are small  
156 (R. Simon, personal communication). We thus conclude that atmospheric forcing is the  
157 most likely candidate to generate the observed oscillations, and we design our modelling  
158 strategy accordingly.

### 3. Model description

159 The GUINEA model developed for this study is based on the primitive equation code  
160 NEMO/OPA.9 developed at LOCEAN (<http://www.lodyc.jussieu.fr/NEMO>). It is a sec-  
161 ond order finite difference model with a free surface, formulated in z-coordinates. The im-  
162 plementation of partial step bathymetry with a new momentum advection scheme has led  
163 to large improvements of the representation of current-topography interactions (*Barnier*  
164 *et al.* [2006], *Le Sommer et al.* [2007]), which makes it a suitable model for our study. The  
165 horizontal grid is a Mercator grid with a resolution  $1/12^\circ$ , covering the Gulf of Guinea  
166 from  $15^\circ\text{S}$  to the Northern African coast near  $5^\circ\text{N}$  and from  $2.5^\circ\text{W}$  to the Eastern African  
167 coast. The vertical grid has 100 levels with 5 m resolution at the surface and 70 m res-  
168 olution below 1500 m. This vertical resolution allows to resolve the strong stratification  
169 in the surface layers of the Gulf of Guinea as well as the currents near the bottom. The  
170 model bathymetry is based on ETOPO2 (*Smith and Sandwell* [1997]) smoothed by ap-  
171 plying twice a Shapiro filter. The vertical mixing is performed by a second order closure  
172 (TKE scheme). Bottom friction is nonlinear, with drag coefficient  $C_d = 1.10^{-3}$ . A hori-  
173 zontal biharmonic operator is used for the lateral mixing of both tracers and momentum  
174 with coefficient equal to  $5.10^9\text{m}^4.\text{s}^{-1}$ . A Laplacian operator with a coefficient equal to  
175  $350\text{m}^2.\text{s}^{-1}$  has been added at the equator (between  $3^\circ\text{S}$  and  $3^\circ\text{N}$ ) in the upper 500 m



176 following *Arhan et al.* [2006]. This additional mixing in the upper equatorial band was  
177 needed to control the strength of the equatorial undercurrent.

178 Open boundary conditions have been applied at the west and south boundaries follow-  
179 ing the method described in *Treguier et al.* [2001]. We added "sponge layers" for the two  
180 boundaries, with an additional Laplacian operator for momentum, to prevent the gener-  
181 ation of spurious eddies. At the boundaries we need data for temperature, salinity and  
182 the velocity component normal to the boundary. Our study of 14-day oscillations requires  
183 high frequency boundary forcing (daily), which can be obtained only from a numerical  
184 model. We believe that it is important to ensure consistency between forcing at the open  
185 boundaries and the surface atmospheric forcing. For this reason we have used a lower res-  
186 olution model ( $1/4^\circ$ ) in a larger domain including the GUINEA model region, and forced  
187 with the same atmospheric data. This model, called NATL, is similar to the one described  
188 in *Le Sommer et al.* [2007], except for a reduced northward extension and the absence  
189 of an ice model. It covers the Atlantic ocean from  $24^\circ\text{S}$  to  $70^\circ\text{N}$  with a  $1/4^\circ$  horizontal  
190 resolution and 46 vertical levels. A special strategy detailed in *Guiavarc'h* [2007] has been  
191 implemented to output daily fields in the region covered by the GUINEA model.

192 Both GUINEA and NATL are initialized using the Levitus climatology. The models are  
193 spun up during 5 years (1995-1999) using the forcing dataset of *Large and Yeager* [2004].  
194 This dataset has been designed for CORE (Coordinated Ocean Reference Experiments)  
195 and includes carefully balanced data from various origins. The daily radiative fluxes  
196 and monthly precipitations are from satellite observations. The 6-hourly temperature,  
197 specific humidity and 10 m winds come from the NCEP/NCAR reanalysis. The turbulent  
198 fluxes are calculated using the CORE bulk formulae. In addition, monthly climatological

199 river runoffs from the study of *Dai and Trenberth* [2002] are implemented as described by  
200 *Bourdalle-Badie and Treguier* [2006]. To avoid a large model drift due to the uncertainties  
201 in the freshwater fluxes, there is a relaxation of sea surface salinity to the LEVITUS  
202 climatology with a coefficient of  $0.25 \text{ m.day}^{-1}$ . The QUIKSCAT satellite scatterometer  
203 produces high quality daily wind fields since 2000 (*Bentamy et al.* [2002]). We prefer  
204 these to the NCEP/NCAR reanalysis winds for our reference experiment (REF) which  
205 is integrated over years 2000-2004 following the spin-up. Humidity, air temperature,  
206 radiative fluxes and precipitations are from the CORE dataset, but turbulent fluxes are  
207 calculated using QUIKSCAT winds in the CORE bulk formulae.

208 The REF experiment has been validated in *Guiavarc'h* [2007]; details are not repeated  
209 here. The surface circulation in the Gulf of Guinea (the Guinea current and the south  
210 Equatorial current) are adequately reproduced, as well as their strong seasonal variability.  
211 In the subsurface, the Equatorial Undercurrent agrees with the observations documented  
212 by *Arhan et al.* [2006] and displays a strong seasonal cycle. In the deep layers, the  
213 circulation is in agreement overall with *Stramma and Schott* [1999] and *Arhan et al.* [2003].  
214 The drifts of salinity and temperature over the 10-years of simulation are relatively weak.  
215 However, the stratification at the equator differs from the climatology. The shallow and  
216 thin thermocline observed in the Eastern Tropical Atlantic is very difficult to capture in  
217 numerical models: in our case it is too deep and too thick, perhaps due to deficiencies in  
218 the forcing field as well as in the parameterization of vertical diffusion.

219 The main objective of the REF simulation is to reproduce the observed biweekly oscil-  
220 lations on the continental slope. In order to investigate their origin, a set of sensitivity  
221 experiments has been carried out by changing wind forcing and/or open boundary forcings

222 from daily to monthly. Our strategy for sensitivity experiments with monthly wind forcing  
223 is the following. We continue to use daily wind speed to calculate turbulent heat fluxes  
224 and evaporation, but we force the momentum equation with a monthly averaged wind  
225 stress calculated from the reference experiment. In this way, we study the effect of high  
226 frequency momentum input by the wind in isolation, without modifying the turbulent  
227 heat flux.

#### 4. Biweekly oscillations in the reference experiment

228 The main characteristics of the variability revealed by the BIOZAIRE data is the bot-  
229 tom intensification, the orientation of currents parallel to the topography, and a kinetic  
230 spectrum dominated by the biweekly frequency. Let us consider how these motions are  
231 reproduced by the REF experiment of the GUINEA model. Fig. 5 presents the velocities  
232 along the local isobath and the variance ellipses for the period around 14-day. Biozaire  
233 data are plotted together with the model velocities at the model grid point closest to the  
234 BIOZAIRE site, for each year (2000-2003). The agreement is good in general. The model  
235 reproduces very well the orientation and the period of the observed currents, although  
236 with a somewhat underestimated amplitude. This is a clear improvement over the ATL6  
237 model, which had a peak-to-peak amplitude 5-10 times smaller than the observations.  
238 Biweekly oscillations are polarized along the bathymetry, except in 2003 when the obser-  
239 vations show a wider ellipse not reproduced by the model. However, the model signal is  
240 not in phase with the observations. Coherences have been computed and vary from 0.43  
241 to 0.72 for the 14-days period band, but are not significant at the confidence level 95%.  
242 Kinetic energy spectra have been computed at model levels close to the depths of the TO-  
243 TAL mooring (Fig. 6). The energy level agrees well with the observed spectra (Fig. 4),

244 confirming the visual impression of the along-slope velocity plots. The model spectra  
245 display a significant peak at all levels at a period close to 14 days, like the observations,  
246 and the bottom intensification is similar. This result is another improvement compared  
247 to the ATL6 model where the 30-day period was more energetic than the 14-day one. At  
248 shorter periods (a few days) the model kinetic energy is larger at the top level (389 m)  
249 than in the deep ocean, a feature that also appeared in the observed spectra.

250 We indicate the values of eddy kinetic energy integrated over the 12-17 days frequency  
251 band in Table 2 for a quantitative comparison with the data. The energy in the model  
252 is slightly lower than the observations both for TOTAL and BIOZAIRE data (except in  
253 2001) but displays a similar interannual variability, with almost a factor of two between  
254 the least energetic year (2002) and the most energetic one (2000). For both model and  
255 data, kinetic energy over the 12-17 days period band represents the half of the total kinetic  
256 energy for subinertial frequencies (between 42 and 63% for the model, between 39 and 47%  
257 for the data). A profile of eddy kinetic energy averaged over 5 years (2000-2004) is plotted  
258 in Fig. 7. Values from TOTAL (year 1998) and Ifremer (two-year average at 410 mab  
259 and four-year average at 30 mab) are indicated for comparison. This figure confirms that  
260 the model captures well the observed bottom intensification of the 14-day signal. The  
261 kinetic energy ratio between the depths 1163 m and 772 m is about 3-5 (according to the  
262 width of the frequency band considered). This is close to the kinetic energy ratio between  
263 1185 m and 785 m for the TOTAL data (2.8-5).

264 It is clear that the high resolution model GUINEA overcomes the major defects of the  
265 ATL6 model considered by *Vangriesheim et al.* [2005]. Various differences between the  
266 models can explain the improved results. First, a better forcing field is used (Quikscat

267 winds) and the representation of bottom topography is made more realistic by a partial  
268 cell formulation (the latter has been found to improve the quality of a global version of  
269 this model by *Barnier et al.* [2006]). These improvements are also present in the larger  
270 domain, lower resolution NATL configuration (which is used to force the open boundaries  
271 of GUINEA). This leads to a better representation of the kinetic energy spectrum: in  
272 both NATL and GUINEA the 14-day period is dominant compared to the 30-day one,  
273 which was not the case in ATL6. Comparison of NATL and GUINEA shows that the  
274 increase in model resolution is necessary to represent the bottom intensification of the  
275 signal (Fig. 7). The very good results of the GUINEA model, which does not include the  
276 tides, confirm that tidal forcing is not necessary to reproduce the observed variability.

277 Note that our results are not strongly dependent on the wind product used for the  
278 forcing. In Fig. 8 the kinetic energy spectrum near the bottom at BIOZAIRE is repro-  
279 duced (black curve, like Fig. 6) and the same spectrum for an experiment with CORE  
280 NCEP winds is indicated (experiment EXP6): there is no significant difference between  
281 the spectra.

## 5. Forcing mechanism of the biweekly oscillations

282 We now use sensitivity experiments to investigate the generation of the oscillations, as  
283 described in Table 3. Over the whole Gulf of Guinea, the wind exhibits 14-day variability  
284 (Fig. 12). The energy is larger in the northern part of the model domain (see Fig. 5 in  
285 *Bunge et al.* [2006]), in agreement with the analysis of *Grodsky and Carton* [2001] and  
286 *Mounier and Janicot* [2004]; however there is 14-day wind variability at the BIOZAIRE  
287 site. Local winds have often been invoked to explain the generation of coastal trapped  
288 waves (*Pizarro and Shaffer* [1998]). To test this hypothesis we have performed EXP1

289 forced by daily winds only in a local box along the African coast (Fig. 1). Elsewhere in  
290 the model, the daily wind stress is replaced by a monthly averaged wind stress computed  
291 from the REF experiment. For the EXP1 sensitivity experiment, there is no evidence of  
292 biweekly oscillations of the deep currents (contrast the red dashed curve in Fig. 8, with  
293 the reference in black). The large difference between EXP1 and REF exists at all depths  
294 for the 14-day frequency band (not shown). It is thus clear that the biweekly oscillations  
295 at BIOZAIRE are not generated by the local winds. On the contrary, in both experiments  
296 REF and EXP1, the kinetic energies at shorter periods (4-5 days) are much more similar.  
297 Local winds certainly play a part in generating the deep near-inertial motions.

298 Biweekly oscillations thus appear to be remotely forced in the model, and the most  
299 likely mechanism is the propagation of perturbations coming from the equatorial wave  
300 guide. This mechanism has been found to generate the intra-seasonal coastal trapped  
301 waves that are observed at the eastern boundary of the Pacific ocean, near the south  
302 American coast. *Shaffer et al.* [1997] describes low frequency fluctuations (50-day period)  
303 off Chile, which can be traced back to Kelvin wave events along the equator. *Enfield et al.*  
304 [1987] analyze oscillations at periods of 1-2 weeks that can be related to equatorial Mixed-  
305 Rossby-Gravity or Yanai waves. Both Kelvin and Yanai waves propagate energy eastward  
306 along the Equatorial wave guide. *Clarke* [1983] has demonstrated that the reflexion prop-  
307 erties of those waves at an eastern boundary are similar; they are partially reflected as  
308 Rossby waves and partially transformed into coastal Kelvin waves, which become coastal  
309 trapped waves in the presence of a bottom slope. With the strong stratification of the  
310 tropical oceans, the properties of coastal trapped waves are close to those of the coastal  
311 Kelvin waves (*Vangriesheim et al.* [2005]). The influence of the equatorial winds on the

312 biweekly oscillations has been explored in the EXP2 experiment (Table 3) where the high  
313 frequency forcing is restricted between  $5^{\circ}\text{N}$  and  $5^{\circ}\text{S}$ . We observe oscillations along the  
314 topography with a peak-to-peak amplitude similar to the REF experiment (not shown).  
315 The kinetic energy spectrum (Fig. 8) exhibits a peak at the same period as REF with  
316 similar amplitude. The model results are compelling evidence that the 14-day oscillations  
317 at the BIOZAIRE location are remotely forced by equatorial winds, in agreement with the  
318 interpretation of similar measurements along the south American coast by *Enfield et al.*  
319 [1987] and *Shaffer et al.* [1997].

320 One may wonder whether it is the wind variability in the Gulf of Guinea itself, or rather  
321 the variability of the winds in the western part of the tropical Atlantic, that is more  
322 important to generate the coastal trapped waves that propagate to the south. Because  
323 GUINEA is a regional model we investigate this question by comparing two experiments,  
324 EXP3 and EXP4 (Table 3). In EXP3 we remove the high frequency winds over the  
325 GUINEA domain, but keep the influence of high frequency forcing outside the domain (we  
326 use monthly winds, but daily open boundary forcing). We do the contrary in EXP4. For  
327 those two simulations, we observe intra-seasonal oscillations oriented along the topography  
328 with similar amplitude, smaller than in REF. This is shown by the kinetic energy spectra  
329 (Fig. 8). We conclude that the energy of the 14-day coastal trapped waves found at  
330 BIOZAIRE is forced to a similar degree by the high frequency winds west of  $2.5^{\circ}\text{W}$ , and  
331 the winds east of that longitude (in the Gulf of Guinea).

332 So far, we have assumed that the biweekly oscillations have been forced by equatorial  
333 winds without taking in account the Tropical Instability Waves (TIW) present in the  
334 Atlantic at intra-seasonal periods. Those waves develop mainly between  $10^{\circ}\text{W}$  and  $25^{\circ}\text{W}$

335 and between 2°N and 5°N (*Caltabiano et al.* [2005], *Grodsky et al.* [2005]), outside the  
336 GUINEA domain at periods between 20 and 40 days. It is quite possible that such  
337 instabilities of the mean currents, rather than direct wind forcing, generate the 14-day  
338 variability that is present in the forcing at the open boundary in REF and EXP3. To test  
339 this possibility we perform experiment EXP5 which is like EXP3, but using daily open  
340 boundary conditions (OBCs) provided by a special NATL experiment forced by monthly  
341 winds. The possible influence of nonlinear instabilities both inside and outside the domain  
342 is thus taken into account in EXP5, unlike experiment EXP1 in which the influence of  
343 TIW was filtered by using monthly OBCs. On the kinetic energy spectra (Fig. 8), we  
344 find that EXP5 (like EXP1) has no peak at 14 days, which confirms that the energy  
345 in that band is directly forced by the wind rather than indirectly by flow instabilities.  
346 This is not true at lower frequencies: indeed for periods longer than 40 days we find that  
347 all experiments with daily open boundaries have similar energy, whether the direct wind  
348 forcing over the GUINEA domain is daily (REF), monthly (EXP3), or a combination  
349 (EXP2 and EXP5). On the contrary, the two experiments with monthly open boundary  
350 forcing (EXP4 and EXP1) stand out with a lower energy level (Fig. 8).

## 6. Propagation and period selection

351 Our sensitivity experiments support the scenario of wind-forced equatorial waves which  
352 then propagate poleward as coastal trapped waves upon reaching the African coast. Let  
353 us examine the characteristics of those equatorial waves in the reference experiment. At  
354 the equator at 0°E, the kinetic energy spectrum at various depths (Fig. 9) shows several  
355 peaks at period around 10, 14 and 35 days, the 35-days peak being the largest (unlike  
356 the kinetic energy spectrum at BIOZAIRE where the 14-days period dominates). Those



357 three peaks at the equator at  $0^{\circ}\text{E}$  agree with the observations of *Bunge et al.* [2006] at  
358  $10^{\circ}\text{W}$ . They carried out spectral analysis of current data between 800 m and 1500 m and  
359 found peaks at 7-day, 14-day, 24-day and 33-day periods. They attributed the 24 and  
360 33-day oscillations to tropical instability waves, but concluded that periods shorter than  
361 20 days were likely wind-forced. The 14-day oscillations had the symmetry characteristics  
362 of Yanai waves, i.e. a signal symmetric with respect to the equator for the meridional  
363 velocity and anti-symmetric for the zonal velocity. To expose the nature of the biweekly  
364 equatorial waves reproduced by GUINEA, we show energy maps for the 14-day period for  
365 both meridional and zonal velocities. To draw these maps (Fig. 10), we have performed  
366 spectral analysis for the two components along the equatorial section at all depths and  
367 extracted the signal for periods between 12 and 17 days. Since currents are much more  
368 energetic near the surface, Fig. 10 shows separately the surface layer and the depths below  
369 200 m. At all depths, the meridional component of the signal is more energetic than the  
370 zonal component. This confirms the results from *Bunge et al.* [2006] that the biweekly  
371 oscillations at the equator are mainly due to Yanai waves (because of their symmetry,  
372 Yanai waves have zero zonal velocity at the equator, while Kelvin waves on the contrary  
373 have zero meridional velocity). In the equatorial Indian ocean, *Miyama et al.* [2006] show  
374 the existence of similar biweekly oscillations due to wind-forced Yanai waves. At biweekly  
375 period, both Yanai and Kelvin waves can exist in the tropical Atlantic ocean (Fig. 13).  
376 Biweekly variability in the atmospheric fields is predominant in the zonal wind stress  
377 component (*Grodsky and Carton* [2001]) and assymmetric compared to the equator (more  
378 energetic north to the equator). So the biweekly variability of the wind stress is mainly  
379 projected into Yanai waves although less energetic Kelvin waves are present near the

380 surface, as appears in Fig. 10. This same figure reveals that the signal is more energetic  
381 in the Eastern part of the domain. This is consistent with the eastward group velocity  
382 of Yanai waves. As shown on Fig. 10, the 14-day signal at the equator has a complex  
383 structure, which will be investigated further in a forthcoming paper. Here, we just note  
384 that an energy maximum is already present at depths of 1000-1300 m at the equator in  
385 the Eastern part of the Gulf of Guinea, and we focus on the propagation of this signal to  
386 the location of BIOZAIRE.

387 Coastal trapped waves generally have a signature at the surface (in the sea surface  
388 height field) so that their propagation has been studied using satellite altimetric data  
389 (e.g., *Lazar et al.* [2006] in the tropical Atlantic). However this is possible only for periods  
390 long compared with the periodicity of the satellite orbit (about 1 week for TOPEX), so  
391 that it is not possible to study the propagation of biweekly waves from observations. A  
392 time-latitude diagram of the meridional velocity along the 1100 m isobath in the GUINEA  
393 model shows clearly a propagation of intra-seasonal waves away from the equator (Fig. 11).  
394 The propagation to the south can be observed beyond the latitude of BIOZAIRE. The  
395 phase velocity computed from this diagram varies from  $c = 0.4 \text{ m.s}^{-1}$  between the equator  
396 and  $3^{\circ}\text{S}$  to greater values between  $0.6 \text{ m.s}^{-1}$  and  $1.5 \text{ m.s}^{-1}$  south of  $3^{\circ}\text{S}$ . Furthermore,  
397 the same figure drawn at several depths shows that the phase speed varies with depth  
398 (not shown). *Vangriesheim et al.* [2005] demonstrated that the  $3^{\text{rd}}$  and the  $5^{\text{th}}$  mode  
399 of CTW were compatible with the 14-day oscillations observed on the continental slope  
400 at BIOZAIRE. Here, the phase velocities computed with the model results indicate that  
401 those biweekly oscillations have complex characteristics and are probably due to a sum of  
402 several mode. The propagation and spatial distribution of those biweekly oscillations will

403 be discussed in a forthcoming paper. Here we simply note that the signal propagation  
404 confirms our sensitivity experiments in pointing out the equatorial origin of the deep  
405 current variability at BIOZAIRE.

406 The remaining question is why the 14-day variability dominates over the other periods  
407 at BIOZAIRE, while the 35-day period dominates at the equator. Let us first consider the  
408 relationship between equatorial currents and equatorial winds. A kinetic energy spectrum  
409 has been computed for the daily QUIKSCAT winds over the latitude band  $5^{\circ}\text{N}$  - $5^{\circ}\text{S}$   
410 (Fig. 12). Three peaks can be distinguished at 35, 14 and 9 days, corresponding to the  
411 dominant periods of the equatorial currents (Fig. 9). This is consistent with a linear  
412 response of the equatorial ocean to the winds, with the ocean acting as a low-pass filter  
413 (in the ocean the 35-day period is more energetic relative to the 14-day period, contrary  
414 to the atmosphere where spectral amplitudes in both bands are similar). Why then is the  
415 biweekly period so dominant at the BIOZAIRE site, with no large peaks corresponding  
416 the 9-day and 35-day maxima found along the equator? The most likely explanation is the  
417 one suggested by *Shaffer et al.* [1997], who have pointed out that for some combinations  
418 of frequency and wavelength, there is no wave propagating energy to the west along  
419 the equator. So for those combinations, all the energy reaching an eastern boundary  
420 propagates as coastal waves (no energy can be reflected westward).

421 We have drawn the dispersion diagram of equatorial waves with parameters appropriate  
422 to the tropical Atlantic (Fig. 13; baroclinic mode velocities have been computed using  
423 the mean stratification between  $5^{\circ}\text{S}$  and  $5^{\circ}\text{N}$ ). The dispersion curves have been drawn for  
424 the first *meridional* mode of equatorial waves but for the first three *vertical* modes. Note  
425 that this is different from dispersion diagrams appearing in *Enfield et al.* [1987], *Shaffer*

426 *et al.* [1997]. Only inertia-gravity waves and Rossby waves can propagate energy to the  
427 west; their dispersion curves are found at the top and bottom of the diagram respectively.  
428 There are no Rossby waves with period smaller than 30 days which is the cut-off period  
429 of the first baroclinic mode. The cut-off period corresponding to inertia-gravity waves is  
430 5 days for the first baroclinic mode but note that it increases for higher vertical modes  
431 (Fig. 13). It reaches 11 days for the fifth mode. For the first five baroclinic modes  
432 together, there is a window between the periods of 11 days and 30 days where there is  
433 no Rossby nor inertia-gravity wave, so that all the energy propagates eastward on the  
434 equatorial waveguide and then poleward as coastal trapped waves. We believe that these  
435 properties of equatorial waves explain why there is a single energy peak around 14 days  
436 at BIOZAIRE, while there are three peaks in the signal at  $0^\circ$  along the equator.

## 7. Discussion

437 In this study we have used a numerical model to show that the biweekly oscillations  
438 observed on the African continental slope at 1300 m depth by *Vangriesheim et al.* [2005]  
439 are remotely forced by equatorial winds. The scenario demonstrated in the model is a  
440 direct forcing of Yanai waves along the equator at all longitudes, followed by poleward  
441 propagation as coastal trapped waves. We believe that this scenario explains the observed  
442 variability, because of the good agreement between the model reference experiment and  
443 the observations at the BIOZAIRE site. We find that the winds in a large equatorial  
444 band ( $5^\circ\text{N}$  to  $5^\circ\text{S}$ ) contribute to the forced response; another experiment with daily winds  
445 restricted to  $2^\circ\text{N}$ - $2^\circ\text{S}$  reproduced only half the energy (*Guiavarc'h* [2007]). This agrees  
446 with the Yanai wave structure of the equatorial response: Yanai waves have a maximum

447 of meridional velocity at the equator, but antisymmetric extrema of zonal velocity on each  
448 side of the equator close to 2°N and 2°S for baroclinic modes 3 to 5.

449 Remote forcing of such coastal-trapped oscillations is not surprising. Propagation of  
450 coastal trapped waves or Kelvin waves away from the equator at intra-seasonal frequency  
451 (around 60 days) appears clearly in satellite altimetry data in the Gulf of Guinea (*Lazar*  
452 *et al.* [2006]). Similar propagation has been demonstrated in the eastern Pacific Ocean  
453 from current meters, altimetry and tide gauges at periods between 10 and 60 days by  
454 *Enfield et al.* [1987] and *Shaffer et al.* [1997], among others. In fact, one may wonder  
455 why such an explanation has not been proposed for the biweekly frequency along the  
456 continental shelf of the Gulf of Guinea, and why the generation by tides has been pre-  
457 ferred in previous studies (*Picaut and Verstraete* [1979], *Clarke and Battisti* [1983]). One  
458 explanation is probably the small number of measurements (moorings and tide gauges)  
459 along the African coast compared with the south American coast, which makes it difficult  
460 to observe poleward propagation from the equator. Another explanation is probably the  
461 lower interannual variability in the Atlantic compared with the Pacific ocean. Observa-  
462 tions of high frequency variability along the south American coast have generally followed  
463 El Nino events, and the authors have been able to relate the increased variability along  
464 the coast to equatorial perturbations. Obviously, the large interannual variability of the  
465 signal in the Pacific ocean makes a tidal origin much less likely. In the Atlantic, although  
466 interannual variability is also present in the biweekly oscillations at the BIOZAIRE site,  
467 the relationship with interannual variability at the equator is not straightforward. In a  
468 forthcoming paper, we try to link the seasonal and interannual variability of the biweekly

469 oscillations to the variability of equatorial winds, and show that the oscillations are more  
470 complex than a simple linear response.

471 The good performance of the GUINEA model in reproducing the major characteris-  
472 tics of the observed variability on the continental slope is very encouraging, and perhaps  
473 unprecedented at such a large depth (1300 m). We have shown that the horizontal and  
474 vertical resolution of the GUINEA model are important to capture the bottom intensifi-  
475 cation and the energy of the signal. We anticipate that three-dimensional ocean general  
476 circulation models will contribute more and more to the study of such coastal trapped  
477 oscillations, because basin scale or even global models with comparable mesh size ( $1/12^\circ$ )  
478 are becoming readily available.

#### 479 **Acknowledgments.**

480 We thank our colleagues of the Laboratoire de Physique des Oceans for their help-  
481 ful advice, and Frederic Marin for his constructive comments and suggestions. Myriam  
482 Sibuet (Ifremer) was the chief scientist of the BIOZAIRE project partly funded by TO-  
483 TAL. Computations presented in this study were performed at the CNRS Institut du  
484 Dveloppement et des Ressources en Informatique Scientifique (IDRIS) in Orsay, France.  
485 TOTAL provided us with additional data\* and financial support: the thesis of Cather-  
486 ine Guiavarc'h has been funded jointly by Ifremer and TOTAL. Annick Vangrieshem is  
487 supported by Ifremer and Anne Marie Treguier by CNRS. We also thank James Richman  
488 and two anonymous reviewers for their constructive suggestions.

489 \*Block 17 Concessionnaire SONANGOL, Sociedade Nacional de Combustveis de An-  
490 gola, EP Sonangol; Esso Exploration Angola (Block 17) Ltd.; BP Exploration (Angola)  
491 Ltd.; Statoil Angola Block 17 A.S.; Norsk Hydro Dezassete A.S.

## References

- 492 Arhan, M., H. Mercier, and Y. Park (2003), On the deep water circulation of the eastern  
493 South Atlantic Ocean, *Deep Sea Research I*, 50, 889–916.
- 494 Arhan, M., A. M. Treguier, B. Bourles, and S. Michel (2006), Diagnosing the annual cycle  
495 of the equatorial undercurrent in the Atlantic Ocean from a General Circulation Ocean  
496 Model, *Journal of Physical Oceanography*, 36, 1502–1522.
- 497 Barnier, B., G. Madec, T. Penduff, J. M. Molines, A. M. Treguier, J. Le Sommer, A. Beck-  
498 mann, A. Biastoch, C. Boning, C. Dengg, J. and Derval, E. Durand, S. Gulev, E. Remy,  
499 C. Talandier, S. Theetten, M. Maltrud, J. McClean, and B. De Cuevas (2006), Impact  
500 of partial steps and momentum advection schemes in a global ocean circulation model  
501 at eddy-permitting resolution, *Ocean dynamics*, DOI: 10.1007/s10236-006-0082-1.
- 502 Bentamy, A., Y. Quilfen, and P. Flament (2002), Scatterometer wind fields : A new release  
503 over the decade 1991-2001, *Can. J. Remote Sensing*, 28, 431–449.
- 504 Bourdalle-Badie, R., and A. M. Treguier (2006), A climatology of runoff for the global  
505 ocean-ice model ORCA025, *Mercator-Ocean report*, MOO-RP-425-365-MER.
- 506 Bunge, L., C. Provost, J. Lilly, M. D’Orgeville, A. Kartavtseff, and J. L. Melice (2006),  
507 Variability of the horizontal velocity structure in the upper 1600m of the water column  
508 on the equator at 10°W, *Journal of Physical Oceanography*, 36, 1287–1304.
- 509 Caltabiano, A. C. V., I. S. Robinson, and L. P. Pezzi (2005), Multi-year satellite observa-  
510 tions of instability waves in the Tropical Atlantic Ocean, *Ocean Science*, 1(2), 97–112.
- 511 Clarke, A. J. (1983), Reflexion of equatorial waves from oceanic boundaries., *Journal of*  
512 *Physical Oceanography*, 13, 1193–1207.

- 513 Clarke, A. J., and D. S. Battisti (1983), Identification of the fortnightly wave observed  
514 along the northern coast of the Gulf of Guinea, *Journal of Physical Oceanography*, *13*,  
515 2192–2200.
- 516 Dai, A., and E. Trenberth, K. (2002), Estimates of freshwater discharge from continents:  
517 latitudinal and seasonal variations, *Journal of hydrometeorology*, *3*, 660–687.
- 518 Enfield, D., M. del Pilar Cornejo-Rodriguez, R. Smith, and P. Newberger (1987), The  
519 equatorial source of propagating variability along the Peru coast during the 1982-1983  
520 El Nino, *Journal of Geophysical Research*, *92(C13)*, 14,335–14,346.
- 521 Garzoli, S. L. (1987), Forced oscillations on the equatorial Atlantic basin during the Sea-  
522 sonal Response of the Equatorial Atlantic Program (1983-1984), *Journal of Geophysical*  
523 *Research*, *92(5)*, 5089–5100.
- 524 Grodsky, S. A., and J. A. Carton (2001), Coupled land/atmosphere interactions in the  
525 West African monsoon, *Geophysical Research Letters*, *28*, 1503–1506.
- 526 Grodsky, S. A., J. A. Carton, C. Provost, J. Servain, J. A. Lorenzetti, and M. J.  
527 McPhaden (2005), Tropical instability waves at 0°N, 23°W in the atlantic: A case  
528 study using Pilot Research moored Array in the Tropical Atlantic (PIRATA) mooring  
529 data, *Journal of Geophysical Research*, *doi:10.1029/2005JC002941*.
- 530 Guiavarc'h, C. (2007), Modelisation haute-resolution des courants dans le Golfe de Guinée:  
531 Etude des oscillations bimensuelles, Ph.D. thesis, Universite de Bretagne Occidentale,  
532 France.
- 533 Houghton, R. W. (1979), Characteristics of the fortnightly shelf wave along the Ghana  
534 coast, *Journal of Geophysical Research*, *84(C10)*, 10,777–10,786.



- 535 Huthnance, J. M. (1978), On coastal trapped waves: analysis and numerical calculation  
536 by inverse iteration, *Journal of Physical Oceanography*, *8*, 73–94.
- 537 Janicot, B., S. and Sultan (2001), Intra-seasonal modulation of convection in the West  
538 African monsoon, *Geophysical Research Letters*, *28*, 523–526.
- 539 Large, W., and S. Yeager (2004), Diurnal to decadal global forcing for ocean sea-ice mod-  
540 els: the data sets and flux climatologies, *NCAR Technical Note: NCAR/TN-460+STR*.  
541 *CGD Division of the National Center of Atmospheric Research*.
- 542 Lazar, A., I. Polo, S. Arnault, and G. Mainsant (2006), Kelvin waves activity in the  
543 Eastern Tropical Atlantic, in *15 years of progress in radar altimetry symposium, Ocean*  
544 *surface Topography Science Meeting. Venice 13-18 March 2006*.
- 545 Le Sommer, J., T. Penduff, S. Theetten, and B. Madec, G. Barnier (2007), How momen-  
546 tum advection schemes influence current topography interactions at eddy permitting  
547 resolution, *submitted to Ocean Modelling*.
- 548 Miyama, T., J. P. McCreary, D. Sengupta, and R. Senan (2006), Dynamics of Biweekly  
549 Oscillations in the Equatorial Indian Ocean, *Journal of Physical Oceanography*, *36*,  
550 827–846.
- 551 Mounier, F., and S. Janicot (2004), Evidence of two independent modes of convection  
552 at intraseasonal timescale in the West African summer monsoon, *Geophysical Research*  
553 *Letters*, *31*, L16,116.
- 554 Picaut, J., and J. M. Verstraete (1979), Propagation of a 14.7 day wave along the northern  
555 coast of the Gulf of Guinea, *Journal of Physical Oceanography*, *9*, 136–149.
- 556 Pizarro, O., and G. Shaffer (1998), Wind-driven coastal trapped waves off the island of  
557 Golland, Baltic Sea, *Journal of Physical Oceanography*, *28*, 2117–2129.

- 558 Shaffer, G., O. Pizarro, L. Djurfeldt, S. Salinas, and J. Rutllant (1997), Circulation and  
559 low-frequency variability near the Chilean coast: Remotely forced fluctuations during  
560 the 1991-1993 El Nino, *Journal of Physical Oceanography*, *27*, 217–235.
- 561 Smith, W. H. F., and D. T. Sandwell (1997), Global seafloor topography from satellite  
562 altimetry and ship depth sounding, *Science*, *277*, 1957–1962.
- 563 Stramma, L., and F. Schott (1999), The mean flow field of the tropical Atlantic Ocean,  
564 *Deep Sea Research II*, *46*, 279–304.
- 565 Treguier, A. M., B. Barnier, A. de Miranda, N. Grima, M. Imbard, C. Le Provost,  
566 G. Madec, C. Messenger, J. M. Molines, S. Michel, and T. Reynaud (2001), An eddy  
567 permitting model of the Atlantic circulation: evaluating open boundary conditions,  
568 *Journal of Geophysical Research*, *106*, 22,115–22,129.
- 569 Vangriesheim, A., A. M. Treguier, and G. Andre (2005), Biweekly current oscillations on  
570 the continental slope of the Gulf of Guinea, *Deep Sea Research I*, *52*, 2168–2183.

<b>Data</b>	<b>Year</b>	$\bar{u}$ (cm.s <sup>-1</sup> )	$\bar{v}$ (cm.s <sup>-1</sup> )	$KE$ (cm <sup>2</sup> .s <sup>-2</sup> )
<b>Ifremer</b>				
890 m (410 mab)	2001	-0.2	-0.4	17
	2002	-0.1	-0.4	21
1270m (30 mab)	2000	1.7	-2.7	43
	2001	0.5	-1.4	28
	2002	0.6	-1.9	21
	2003	0.4	-1.6	24
<b>Total</b>				
385 m	1998	0.3	-0.4	19
585 m	1998	-0.1	-0.4	14
785 m	1998	-0.5	0.2	13
985 m	1998	0.6	-0.4	19
1185 m	1998	0.4	0.1	23
1370 m	1998	0.9	-1.1	23

**Table 1.** Current Statistics at the BIOZAIRE site A. Ifremer data for years 2000-2002 are reproduced from *Vangriesheim et al.* [2005]; data from year 2003 and TOTAL have not been published before. The measurement depth are indicated in meters above bottom (mab) for the Ifremer mooring (total depth is 1300 m). The mean velocities are indicated in the zonal ( $\bar{u}$ ) and the meridional ( $\bar{v}$ ) directions. The eddy kinetic energy (KE) is calculated from the filtered time series, using a Lanczos filter with cut-off period of 6 days.

	Model			Data		
Year	14-day KE	total KE	Ratio	14-day KE	total KE	Ratio
1998	6.2	14.8	42	9.7	23	42
2000	11.0	17.6	63	19.5	44	44
2001	10.8	18.8	57	10.0	25	40
2002	5.7	11.7	49	8.4	22	39
2003	7.1	12.0	59	12.2	26	47

**Table 2.** Kinetic energy (KE,  $\text{cm}^2 \cdot \text{s}^{-2}$ ) in the frequency band 12-17 days (14-day KE) and for subinertial frequencies (total KE), in the GUINEA model and in observations. For the model the KE is calculated at the level above the model bottom layer (135 mab). For the observations, the KE is calculated at 30 meters above the bottom except in 1998 (15 mab). The ratio represents the percentage of the 14-day kinetic energy compared to the total kinetic energy.

Experiment	Wind forcing	Open boundaries
REF	daily	daily
EXP1	daily, 10°E-14°E, 2°S-15°S	monthly
EXP2	daily, 5°S-5°N	daily, 5°S-5°N
EXP3	monthly	daily
EXP4	daily	monthly
EXP5	monthly	daily from NATLM
EXP6	6-hourly NCEP winds	daily

**Table 3.** Sensitivity experiments carried out with the GUINEA model. All experiments cover years 2000-2004 following a common spin-up. Open boundary conditions come from a NATL experiment using the same daily forcing as REF, excepted for EXP5 which uses the NATLM experiment forced by daily heat and freshwater fluxes but monthly wind stress.

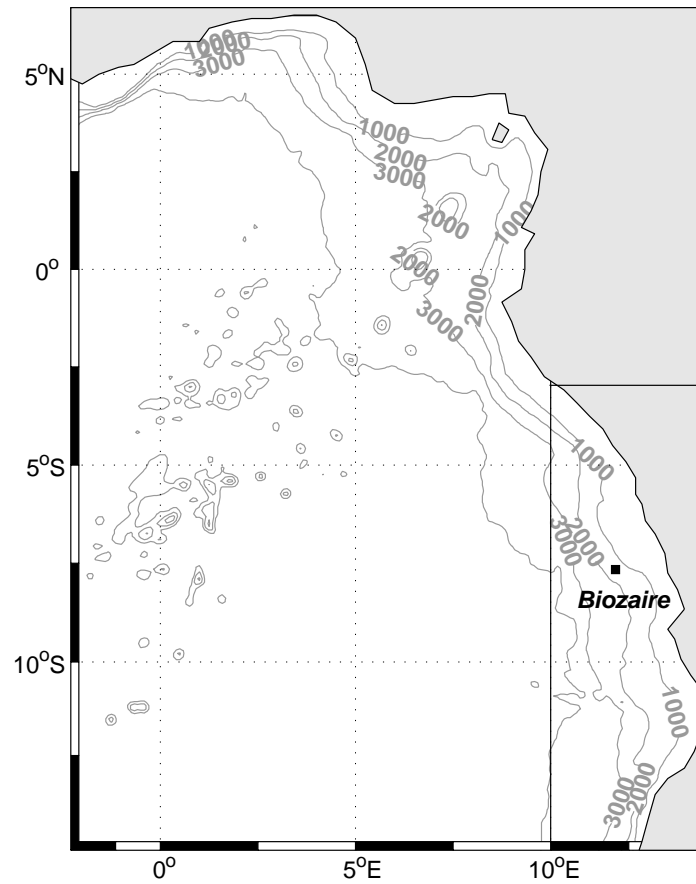


**Figure 1.** Bathymetry of the Gulf of Guinea and position of the BIOZAIRE mooring (Site A:  $7^{\circ}20'S, 11^{\circ}30'E$ ). The TOTAL mooring (not shown on this map) is located at  $7^{\circ}40'S, 11^{\circ}40'E$ , 40 km SSW of the BIOZAIRE mooring at similar depth. The region shown is the domain covered by the GUINEA model. The box corresponds to the local box for daily wind forcing used in experiment EXP1 (Table 3).

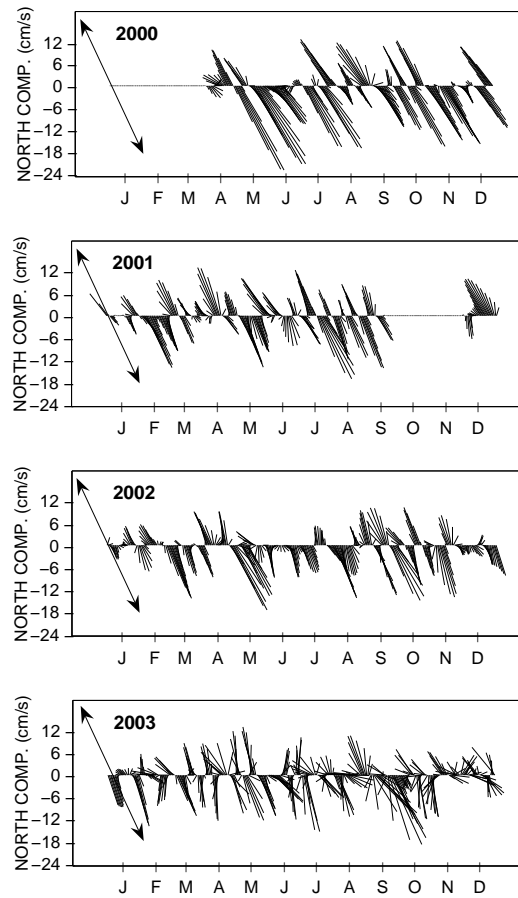


**Figure 2.** Stick plots of velocities at the BIOZAIRE mooring at 30 meters above the bottom (1270 m depth). The arrow indicates the direction of the local isobaths. Data are filtered using a Lanczos filter with a cut-off period of 6 days.

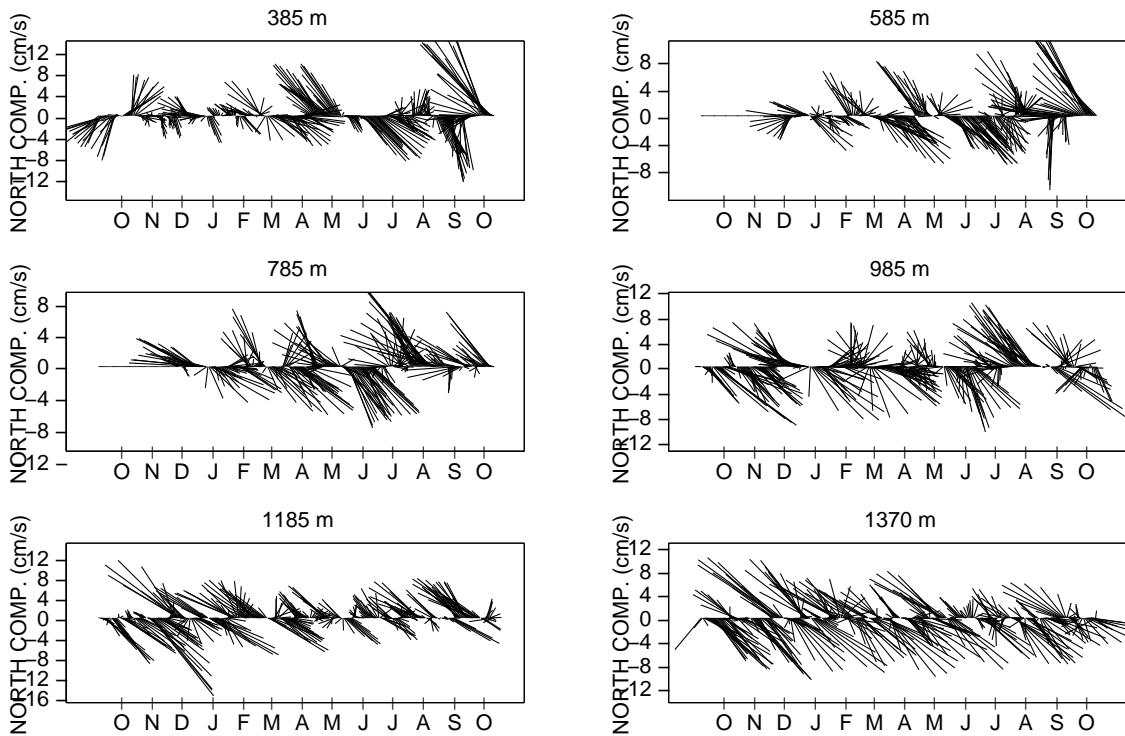


**Figure 3.** Stick plots of velocities at the TOTAL mooring at different depths. Data are filtered using a Lanczos filter with a cut-off period of 6 days.

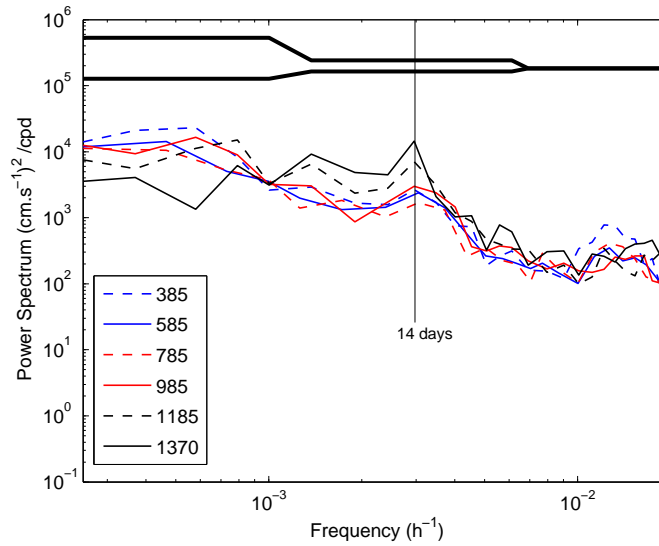


**Figure 4.** Kinetic energy spectra at different depths for the TOTAL mooring. The vertical spacing between the bold lines corresponds to 95% confidence interval.



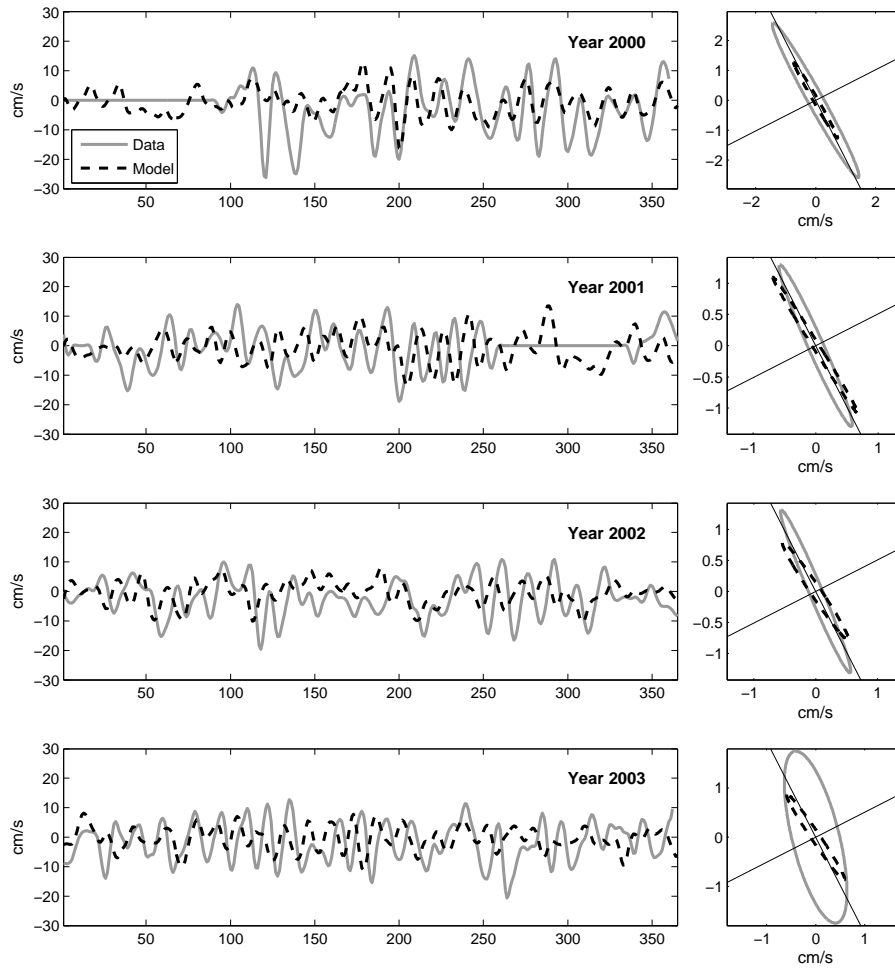


**Figure 5.** Left: Filtered velocity along the bathymetry on the site BIOZAIRE at 30 mab for the data, and at the level above the model bottom layer. Right: Variance ellipses for filtered series in the frequency band around 14 days. The directions parallel and perpendicular to the topography are indicated by thin lines. Model and observed velocities are filtered using a Lanczos filter with a cut-off period of 6 days.

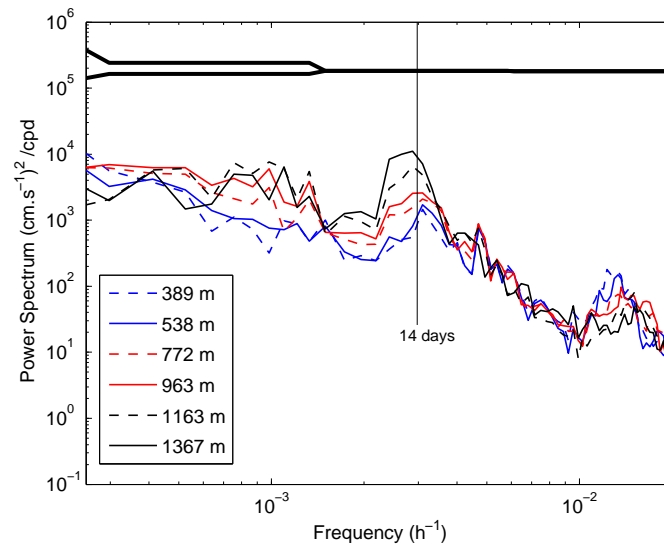


**Figure 6.** Kinetic energy spectra at the BIOZAIRE location in the reference experiment of the GUINEA model at model levels close to the depths sampled by the TOTAL mooring. The vertical spacing between the bold lines corresponds to 95% confidence interval.

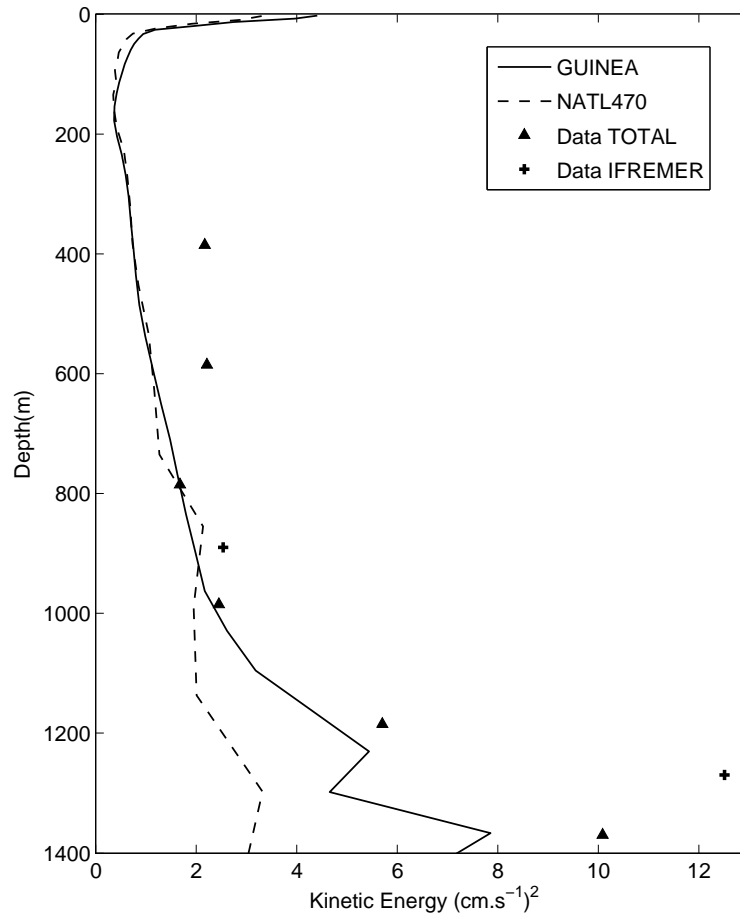


**Figure 7.** Kinetic energy at period between 12 and 17 days at BIOZAIRE site for the TOTAL and Ifremer data, for the REF experiment of GUINEA and for the NATL model.

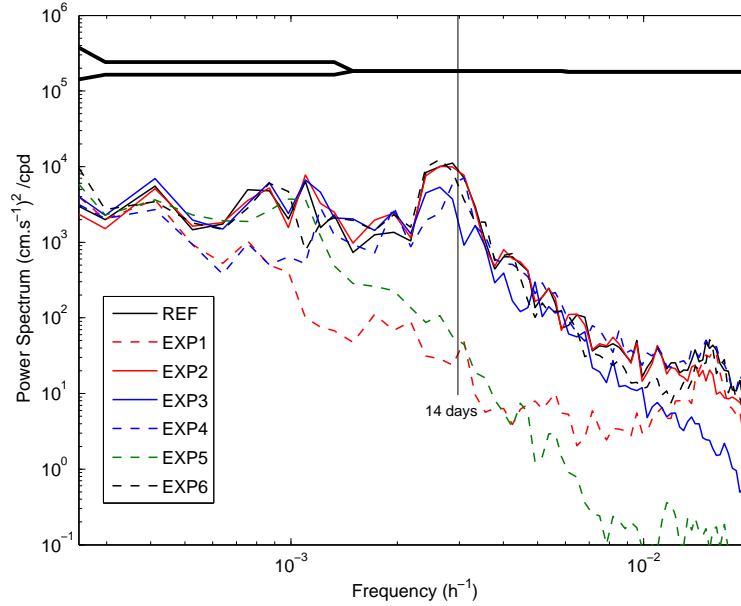


**Figure 8.** Kinetic energy spectra at the BIOZAIRE location in the GUINEA model (deepest model level) in the experiments described in table 3. REF: daily winds OBCs (Open Boundary Conditions); EXP1: daily winds between 10°E - 14°E, 2°S - 15°S and monthly OBCs; EXP2: daily winds and OBCs between 5°S - 5°N; EXP3: monthly winds and daily OBCs; EXP4: daily winds and monthly OBCs; EXP5: monthly winds and daily OBCs from NATLM; EXP6: 6-hourly CORE winds and daily OBCs.

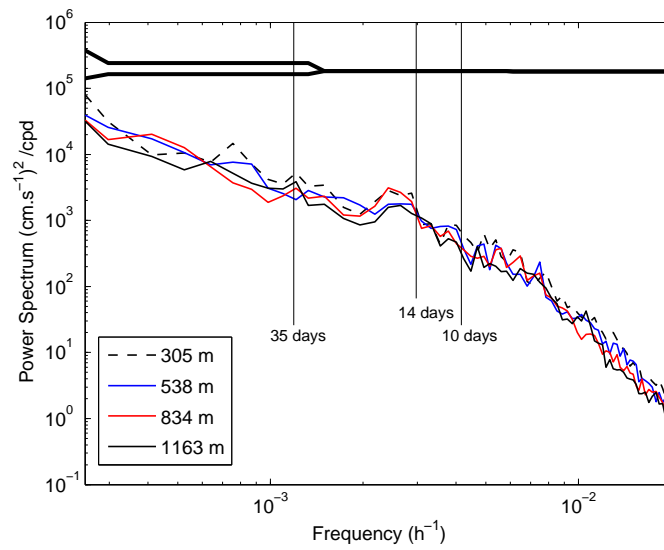


**Figure 9.** Kinetic energy spectra at the equator at  $0^\circ\text{W}$  in the reference experiment of the GUINEA model at several levels. The vertical spacing between the bold lines corresponds to 95% confidence interval.

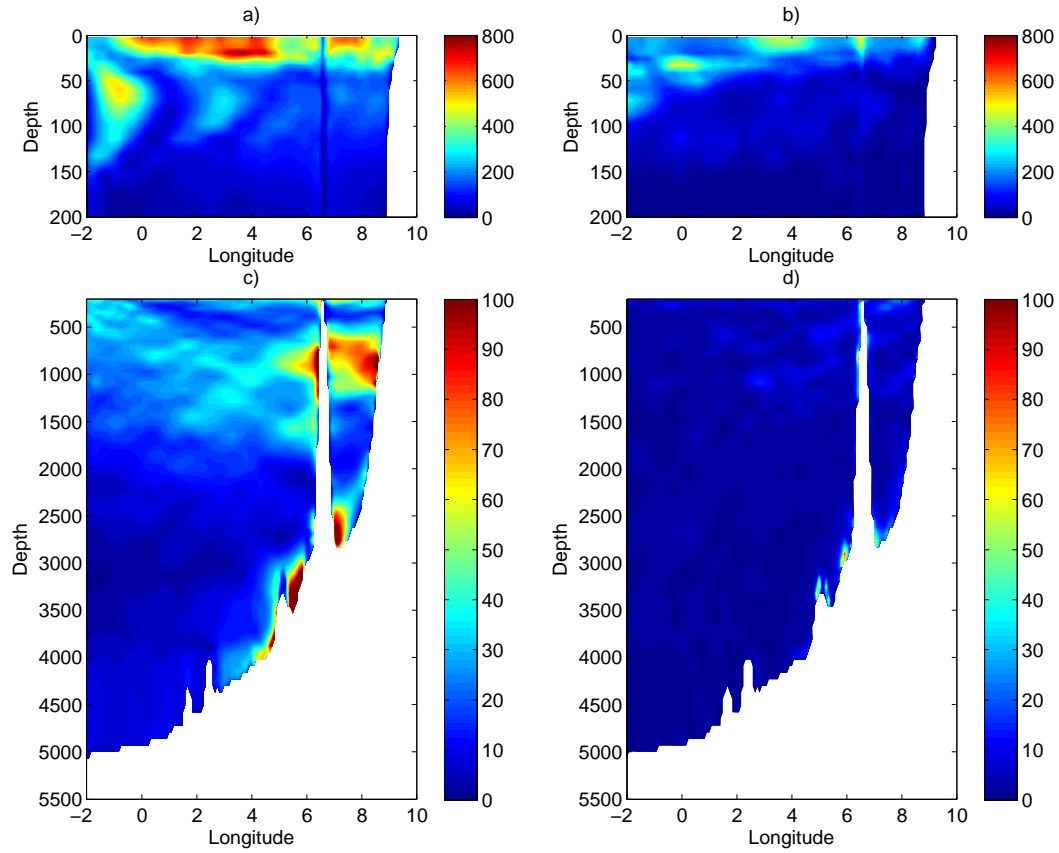


**Figure 10.** Kinetic energy (cm<sup>2</sup>.s<sup>-2</sup>) at periods between 13 and 16 days at the equator in the reference experiment. a) and b): upper layers above 200 m, for the meridional and for the zonal component. c) and d): below 200 m for the meridional and for the zonal component, respectively.

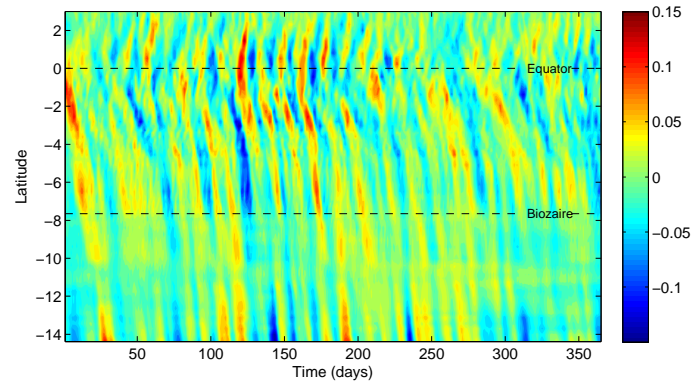


**Figure 11.** Time-latitude plot of the meridional velocity along the isobath 1100 m in the REF experiment of the GUINEA model.

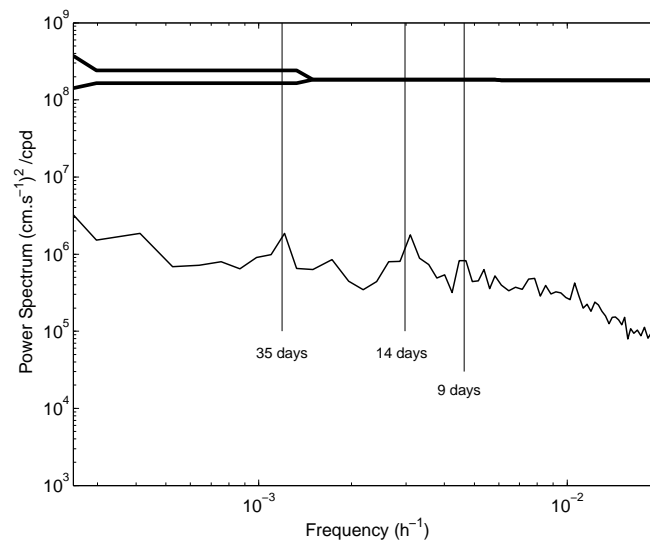


**Figure 12.** Kinetic energy spectra for the QUIKSCAT winds averaged over the GUINEA domain between 5°S and 5°N. The vertical spacing between the bold lines corresponds to 95% confidence interval.

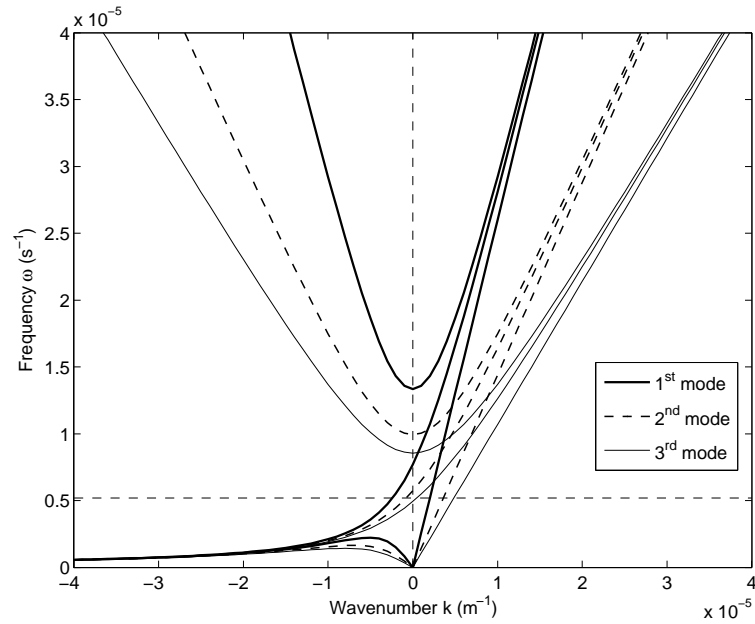


**Figure 13.** Dispersion relations for the first meridional mode equatorial trapped waves in the Atlantic ocean. Curves are drawn for the first three baroclinic modes. Baroclinic mode velocities have been computed using the mean stratification in the Atlantic ocean between  $5^{\circ}\text{N}$  and  $5^{\circ}\text{S}$ . The velocities are equal to 2.35 m/s, 1.35 m/s and 0.92 m/s for the 1<sup>st</sup>, 2<sup>nd</sup> and 3<sup>rd</sup> baroclinic mode, respectively. The horizontal dashed line indicates the 14-day period.